International Research Journal of Engineering and Technology (IRJET) e-ISSN: 2395-0056
Volume: 11 Issue: 01 | Jan 2024 www.irjet.net p-ISSN: 2395-0072

Augmentation of Multimodal 3D Magnetic Resonance Imaging using Generative Adversarial Network for Brain Tumor Segmentation

Bhavesh Parmar[1, 2], Mehul Parikh[2]

[1]*Research Scholar, Gujarat Technological University, Gujarat, India*
[2]*L. D. College of Engineering, Ahmedabad, Gujarat, India*

Abstract – *Gliomas are the most common malignancy in brain. Magnetic Resonance Imaging (MRI) images are widely used for medical imaging applications. Multimodal MRI can be used effectively for segmentation of brain tumors using Convolutional Neural Network (CNN). CNN accuracy depends on the large amount of data. Medical imaging datasets are mostly smaller in size. There is a chance of missing modality in MRI due to clinical settings or in case of patient not available for prognosis. This paper proposed a novel generator – discriminator architecture for development of cohort of MRI modality. Modified 3D UNet architectures were used as generator and PatchGAN for discriminator. In BraTS2020 dataset, there are four MRI modalities present. The modified 3D Unet provided with different three modalities as input and it produce the remaining modality. Discriminator block find the MSE, PSNR, and SSIM values to check before adopting as cohort. The generated modalities are used as input along with the original images in dataset for input to the modified 3D Unet. The model performance in segmentation improved up to 2 to 3 points in each tumor sub regions. The mean dice values achieved using the proposed work is 0.87. 0.81. and 0.78 for WT, TC, and ET respectively.*

1. INTRODUCTION

Magnetic Resonance Imaging (MRI) is the widely used imaging modality in the clinical practice. MRI can be very useful in assessing different insights in diagnosis and clinical planning. Multimodal characteristics of MRI scans can be very useful in neuroimaging, specifically brain tumor classification and segmentation. Gliomas are the most frequently occurring central nervous system (CNS) malignancy accounting 30% to all other CNS tumors [1]. World Health Organisation (WHO) classified brain tumors in grade I to IV considering aggression of malignancy. With amplifying order of antagonism, Grade I and II are Low Grade Glioma (LGG), while, grade III and IV are High Grade Glioma (HGG) [2]. Due to very high variations in size, shape, structure, infiltrative nature of growth and peritumoral edema, brain tumors are hard to delineate from its surrounding healthy tissues. Further, the large volume of MRI scan, Manual border segmentation with visual inspection is time consuming and prone to human error [3].

Recently, deep learning methods have shown promising results in medical imaging [4]. 3D UNet [5] and variations of 3D UNet [6-9] are the most adopted method for brain tumor segmentation applications.

Model accuracy in segmentation for the deep learning network is data centric. Medical Imaging dataset are usually smaller in comparison to other computer vision datasets. The requirement of multimodal patient imaging might also not possible due to various clinical requirements. Additionally, prognosis and follow up of singular subject may not be possible. To cater the need, unavailable image data can be augmented using Generative Adversarial Network (GAN).

In this paper, generative and discriminative method of GAN is proposed and compared its suitability and improvements in outcomes on existing methods of brain tumor segmentation application.

2. RELATED WORKS

Due to success of deep learning in compute vision applications, data demand increasing day by day [10]. Unlike other computer vision dataset, medical imaging datasets are limited. The need of augmented data can solve the problem of inadequate dataset. Various application of GAN includes image to image translation [11], image synthesis from noise [12], style transfer [13], and image segmentation [14]. Due to smaller size of medical image datasets, GAN algorithms are getting popularity.

The Generative Adversarial Network (GAN) method was originally introduced in 2014, by Good fellow et al [10], for image generation. In Medical image synthesis, CycleGAN can be helpful for cohort of absent modalities [15]. GANS can also be used for segmentation of medical images. Han et al., has suggested GAN method for multiple spinal structure segmentation from MRI scans. Several methods suggested possibility of utilizing GAN in medical image segmentation [11, 16, 17, 18]. Another 2D GAN based method RescueNet was proposed for brain tumor segmentation from MRI images [19]. The detailed review of application of GAN is reviewed by Yi et al [20].

This work is motivated from the MM-GAN [21], a 3D extension of Pix2Pix GAN [22]. The method synthesise missing image of modality from the by the available images of another three modalities in multimodal brain tumor

segmentation application. The modified patch based 3D UNet [23] along with PatchGAN [24] proposed here for Generator-Discriminator framework to improve the segmentation accuracy in brain tumor segmentation application using BraTS2020 [25-29] dataset.

3. METHOD

3.1 Data

The BraTS2020 dataset were used for this work. Multimodal Brain Tumor Segmentation (BraTS} challenge consisting of MRI scans of 240 x 240 size with 155 scans in each slice [25]. BraTS2020 dataset includes 369 training data of different subjects collected from different scanner and protocols at various institutions [26-29]. It includes four modalities of MRI namely; (i) T1 – native scan, (ii) T1ce – Post contrast T1 weighted, (iii) T2 – T2 weighted, and (iv) FLAIR – T2 Fluid Attenuated Inversion Recovery. Another 125 and 166 previously unknown subject data of all four modalities were provided for validation and testing [29]. Training data were manually segmentated and approved by experienced neurologist. Figure 1 Show the sample scan of different MRI modalities from the data set.

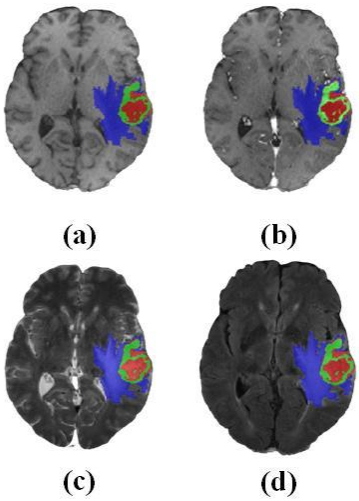

Fig -1: MRI modalities in transverse plane overlapped with ground truth segmentation for (a) T1, (b) T1ce, (c) T2, and (d) FLAIR, indicated with colour blue, green and red for Peritumoral edema (ED), necrotic and non-enhancing tumor core (NCR/NET), and GD-enhancing tumor (ET) respectively.

Multimodal nature of MRI can be useful in tumor sub region segmentation and the qualitative visuals of each modality are in figure 1. MRI volumes in transverse, coronal and sagittal anatomical planes are displayed in figure 2 with corresponding ground truth of tumor regions.

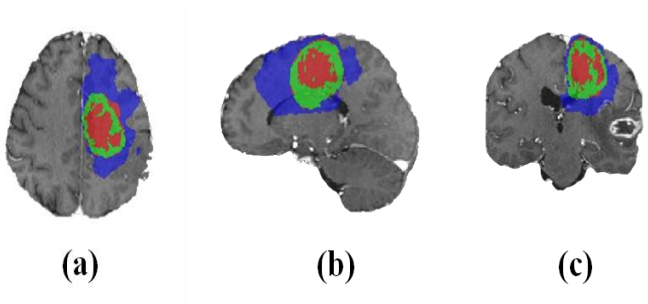

Fig -2: MRI scans in (a) transverse, (b) coronal, and (c) sagittal plane for a typical sample images from the BraTS2020 dataset.

3.2 Data Pre-processing

BraTS2020 provides rigidly registered scans with skull-stripping and, resample at $1mm^3$ isotropic resolutions. The multi institutional and different protocol in MRI image acquisition creates nonlinearity in images. There is intensity variation in MRI scans while recording. These inherent intensity inhomoginities can be removed using N4ITk insight toolkit [30]. Min-Max scaling applied to standardise the dataset in the range of 10 to 110 voxel intensity values. Further, using mean and standard deviation values of intensity of voxel, z-score normalisation were applied between 0 and 1 for each voxel before feeding to the network.

To prevent overfitting of the model during training, 3D mirroring, random 3D rotation between 0 to 45° and random elastic deformation were applied with 50 % probability of combination of augmentation.

3.3 Model Architecture

The overall architecture of the proposed method is displayed in figure 3. The framework includes two blocks; Generator for development of synthetic image and discriminator for comparing the output with ground truth.

The generator is an encoder-decoder based architecture, a modified 3D UNet architecture with concatenated skip connections [23]. In the Downsample block consist of convolution, batch Normalization and leaky ReLU. Convolution is performed on input through several filters with fixed kernel size 4 and stride 2. Batch normalization prevents vanishing gradient and leaky ReLU used as an activation function. The Upsampling block made of four layers, transposed Convolution, Batch Normalization, Dropout, and ReLU. In transposed convolution, image is stitched and convolved to enlarge the size. Dropuout is useful in preventing overfitting, and ReLU is used as activation function which stops the saturation. The framework of generator block is shown in figure 3, with all the sub-blocks included in Downsampling and Upsampling blocks.

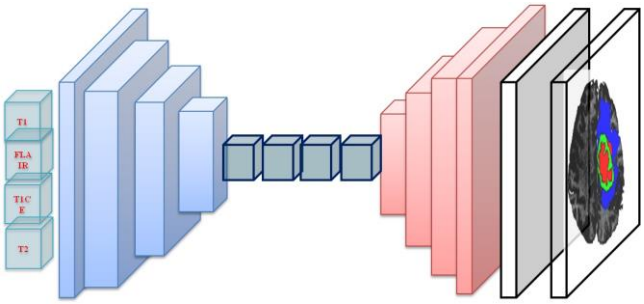

Fig -3: Generator framework with encoder decoder architecture, consisting of downsampling and upsampling blocks on both side respectively.

The discriminator is PatchGAN [24] consisting of four discriminating blocks followed by zero padding and convolution. Each discriminating blocks composed of Convolution, Batch Normalization, and Leaky ReLU. The convolution in discriminator block having filters from size 60 to 512 and Batch normalization applied after the first block. Convoluting is performed after discriminative block followed by zero padding, with kernel size 4 and stride 1. The discriminator framework is displayed in figure 4.

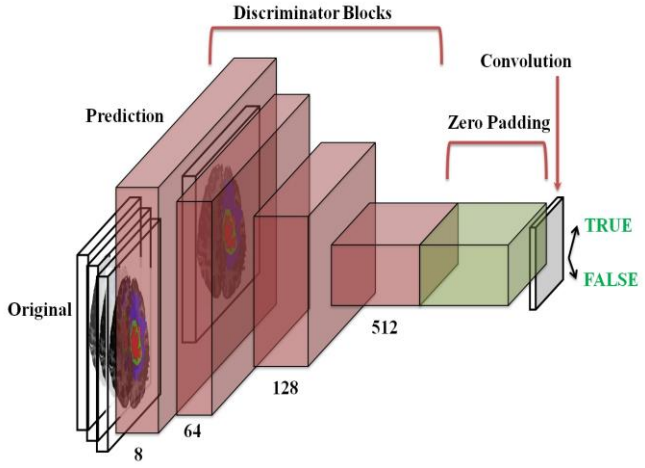

Fig -4: Discriminator framework with four discriminator blocks followed by zero padding and convolution, giving binary output

3.4 Losses

The generator and discriminator architecture use loss function as suggested in [22], written as loss;

$$\mathcal{L}_G \leftarrow \lambda\mathcal{L}_1(G(x), y) + (1-\lambda)\mathcal{L}_2\big(D(x, G(x))\mathcal{L}_{ar}\big) \quad (1)$$

$$\mathcal{L}_D \leftarrow \mathcal{L}_2\big(D(x, G(x))\mathcal{L}_{ar}\big) + \mathcal{L}_2\big(D(x, G(x))\mathcal{L}_r\big) \quad (2)$$

Where *x* is concatenation of three inputs sequence and *G(x)* symbolize guess generated by GAN. Dummy loss function $\mathcal{L}_{ar}$ generated with all values one, used by generator loss $\mathcal{L}_1 and\ \mathcal{L}_2$ are L_1 norm (absolute error) and L_2 norm (mean square error) respectively. $\mathcal{L}_r$ *is* used as null tensor.

4. RESULTS

4.1 Implementation Details

Pytorch [31] and TensorFlow [32] are implemented using python 3.6 to implement the proposed algorithm. NVIDIA Quadro P5000 GPU 64 bit RAM computing system used for training, validation and testing of model. The 3D UNet network was initially trained on 295 images with 80:20 rations for training and validation. Later the network was trained on 369 images, followed by validation on 125 images and tested on 166 unknown images from BraTS dataset. Dice Similarity score, simply known as dice, and Hausdorff distance (95th percentile) were evaluated.

4.2 Evaluation Parameters

Augmentation Quality

The first metrics we considered aim at assessing the quality of the whole images generated. To compute these metrics we first had to crop and normalize the images as follows. We center-cropped the generated images to 155x194, which is the size of the largest bounding box to contain each brain in the BraTS2015 dataset [26]. Then, we applied mean normalization [33] to each image for generated or real, and computed the following three metrics: (i) the mean squared error (*MSE*), (ii) the Peak Signal-to-Noise Ratio (*PSNR*) [34], and (iii) the Structural Similarity (*SSIM*) [35]:

$$MSE(\hat{I}, I) = \frac{1}{W \cdot H}\sum_{i=1}^{W}\sum_{i-1}^{H}\big(\hat{I}_{i,j} - I_{i,j}\big)^2 \quad (3)$$

$$PSNR(\hat{I}, I) = 10log_{10}\frac{\big(max(\hat{I}_{i,j})\big)^2}{MSE(\hat{I}, I)} \quad (4)$$

$$SSIM(\hat{I}, I) = \frac{(2\mu(I) + \mu(\hat{I}) + c_1)(2\sigma(\hat{I}, I) + c_2)}{(\mu^2(I) + \mu^2(\hat{I}) + c_1)(\sigma^2(I) + \sigma^2(\hat{I}) + c_2)} \quad (5)$$

Where, *W* and *H* are the width and height of the images. *I* and $\hat{I}$are the real and generated image respectively. $I_{i,j}$, and $\hat{I}_{i,j}$ are the pixel values of respectively the real and generated images; μ is the average of pixel values, σ^2 is the variance of pixel values, and $\sigma(\hat{I}, I)$is the covariance of $\hat{I}$and *I* pixel values. Both *MSE* and *SSIM* have values between 0 and 1. Lower values of MSE mean a better quality of the generated image. Instead, the greater the SNR and SSIM are, the better is the quality.

Model Performance

Evaluation of segmentation performance can be measured with the Sorensen–Dice index also known as the Dice Similarity Coefficient (DSC) of simply Dice [35]. DSC represents the degree of overlap between predicted region map and ground truth and calculated using equation 5 as;

$$DSC = \frac{2TP}{FP + 2TP + FN} \quad (6)$$

Where, notations TP, FP and FN are True Positive (TP), False Positive (FP) and False Negative (FN) respectively.

Hausdorff distance measures the maximum distance of one set to the nearest point in the other set [18], defined as:

$$D_H(P,Q) = max\left\{\left(sup_{x\epsilon P} inf_{y\epsilon Q} d(x,y)\right), \left(sup_{y\epsilon P} inf_{x\epsilon P} d(x,y)\right)\right\} \quad (7)$$

Where, *sup* and *inf* represents the supremum and the infimum among the considered sets. Hausdorff distance at 95th percentile (HD95) is considered to avoid noisy segmentation and achieve more robust results the evaluation scheme uses the 95th percentile.

4.3 Augmentation Evaluation

Three MRI sequences given as input to the generator network and the output are passed through the discriminator. i.e. T1ce, T2, and FLAIR input given for generation of T1 scan. Four such experiments were performed to find all the missing modality generation in the current scenario. The passes outcome is evaluated with MSE, PSNR, and SSIM for whole brain MRI scan. The MSE and PSNR parameters also been calculated for tumor regions. Table 1 and 2 demonstrates the results for different modalities for values of evaluation parameters for whole image and tumor region respectively.

Table -1: Evaluation of augmented whole image

Modality	MSE	PSNR	SSIM
T1	0:0041 ± 0:0038	25:2569 ± 3:6512	0:8472 ± 0:0830
T1CE	0:0054 ± 0:0040	23:9242 ± 3:6958	0:8027 ± 0:1003
T2	0:0077 ± 0:0061	22:3719 ± 3:5290	0:7835 ± 0:1141
FLAIR	0:0072 ± 0:0050	22:5524 ± 3:5655	0:7610 ± 0:1175

Table -2: Evaluation of tumor region from augmented image

Modality	MSE	PSNR
T1	0:0113 ±0:0099	20:8938 ± 3:6111
T1CE	0:0168 ± 0:0172	19:8441 ± 4:6258
T2	0:0207 ± 0:0167	18:1305 ± 3:5930
FLAIR	0:0221 ± 0:0375	19:0374 ± 4:1582

Lower values of MSE mean a better quality of the generated image. Instead, the greater the SNR and SSIM are, the better is the quality. Mean value of MSE for the generated modalities as displayed in table 1 is evident that the performance of GAN method proposed here is acceptable. All three parameters indicate almost equal behaviour for all modalities. The similarity of T1 and T1ce considered being better to T2 and FLAIR images. The variation in the results may be due to class imbalance in the input dataset and the inherent radiomic properties of images. The results might be improved on consideration of only two related modalities instead of three input channel considered here.

The dice similarity coefficient (DSC) also referred as dice and Hausdorff distance (95th Percentile) were calculated from ground truth and the synthesized image to find the applicability of proposed method in the brain tumor segmentation. Table 3 demonstrate the performance of model trained with synthetic MRI scans in training, validation and Testing and table 4 compared with the existing state-of-the art methods.

Table -3: Performance of model using synthetic MRI scans,

Method	Dice			Hausdorff (mm)		
	WT	TC	ET	WC	TC	ET
Train	0.91	0.89	0.79	3.66	3.52	30.04
Valid	0.89	0.79	0.75	6.39	14.07	36.00
Test	0.87	0.81	0.78	6.44	24.36	18.95

The mean values of Dice and Hausdorff represents the performance of modified 3D Unet network model of synthetic images of each modality generated using the proposed method. The values in test phase are low, which can be considered as the actual performance on unknown dataset. The dice and Hausdorff values are comparatively declining in TC and ET region respectively, due to tissue infiltration in the input images.

Table-4: Performance comparison with state-of-the art methods.

Method	Dice			Hausdorff (mm)		
	WT	TC	ET	WC	TC	ET
3D UNET [6]	0.84	0.83	0.76	7.37	11.15	26.78
Modified 3D Unet [23]	0.83	0.82	0.74	5.34	11.34	23.29
Proposed Method	0.87	0.81	0.78	6.44	24.36	18.95

The proposed method is compared with most adopted Convolutional Network (CNN) architecture basic 3D Unet and modified 3D Unet. The method considered in this work also use modified 3D Unet. For comparison, in the 3D Unet and modified 3D Unet, the input provided without any modification of original dataset. Whereas the proposed

method takes input of original dataset along with synthetic data, which makes the data size double fold here. The improvement in the results for dice values 0.87, 0.81, and 0.78 for WT, TC, and ET respectively, due to increase in the data size.

The qualitative result of each of the modality is representing in figure 5 as a sample for one of the subject from the dataset.

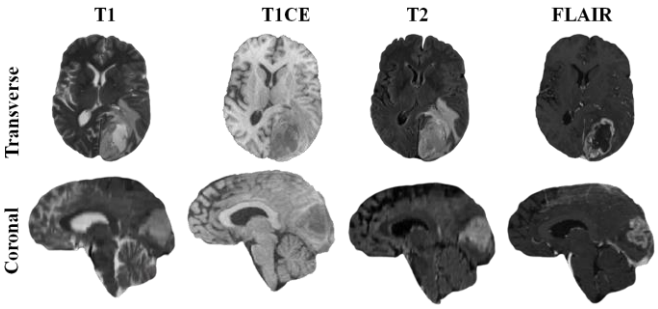

Fig -5: MRI modalities generated from the proposed framework, displayed in transverse and coronal plane.

5. CONCLUSIONS

Generator-discriminator framework from synthesis of MRI imaging modality has been discussed. IN the suggested method, the generator use modified 3D Unet architecture. In BraTS2020 dataset, four modalities are included namely; T1, T1CE, T2, and FLAIR. The generator network fed with any three images of different modality and it produce the remaining modality image as an output. The discriminator use PatchGAN framework and distinguish the output from the available ground truth. Three parameters, MSE, PSNR, and SSIM used to find the suitability of outcome. The image developed with this framework show low mean value of MSE and higher values of PSNR and SSIM. The results suggest to adopt the synthetic image can be considered as cohort of input image. Further, the generated images of different modalities are used along with the original dataset for brain tumor segmentation application using Modified 3D Unet. By making the data volume double, with original and synthetic data, performance of the model improved with dice value of 0.87. 0.81. and 0.78 for WT, TC, and ET respectively.

REFERENCES

[1] Sontheimer, H. (2020). Brain Tumors. *Diseases of the Nervous System (Second Edition)*, 207-233. https://doi.org/10.1016/B978-0-12-821228-8.00009-3.

[2] Wesseling, P., & Capper, D. (2018). WHO 2016 Classification of gliomas. *Neuropathology and applied neurobiology*, *44*(2), 139–150. https://doi.org/10.1111/nan. 12432.

[3] Blystad, I., Warntjes, J. B., Smedby, O., Landtblom, A. M., Lundberg, P., & Larsson, E. M. (2012). Synthetic MRI of the brain in a clinical setting. *Acta radiologica (Stockholm, Sweden : 1987)*, *53*(10), 1158–1163. https://doi.org/10. 1258/ar.2012.120195.

[4] Illimoottil, M., & Ginat, D. (2023). Recent Advances in Deep Learning and Medical Imaging for Head and Neck Cancer Treatment: MRI, CT, and PET Scans. *Cancers*, *15*(13). https://doi.org/10.3390/cancers15133267

[5] Çiçek, Ö., Abdulkadir, A., Lienkamp, S.S., Brox, T., Ronneberger, O. (2016). 3D U-Net: Learning Dense Volumetric Segmentation from Sparse Annotation., *Springer LNCS*, vol 9901. https://doi.org/10.1007/978-3-319-46723-8_49

[6] Myronenko, A. (2019). 3D MRI Brain Tumor Segmentation Using Autoencoder Regularization. *BrainLes 2018*. *Springer LNCS*, vol 11384., 311 – 320, https://doi.org/10.1007/978-3-030-11726-9_28.

[7] Isensee, F., Jaeger, P. F., Kohl, S. A. A., Petersen, J., & Maier-Hein, K. H. (2021). nnU-Net: a self-configuring method for deep learning-based biomedical image segmentation. *Nature methods*, *18*(2), 203–211. https://doi.org/10.1038/s41592-020-01008-z.

[8] McKinley, R., Meier, R., Wiest, R. (2019), Ensembles of Densely Connected CNNs with Label Uncertainty for Brain Tumor Segmentation. *BrainLes2018, Springer LNCS,* 11384, vol. 456–465, https://doi.org/10.1007/978-3-030-11726-9_40.

[9] Zhou, C., Chen, S., Ding, C., Tao, D. (2019), Learning Contextual and Attentive Information for Brain Tumor Segmentation. *BrainLes2018, SpringerLNCS,* vol., 11384, 497–507, https://doi.org/10.1007/978-3-030-11726-9_44.

[10] Goodfellow, I., Pouget-Abadie, J., Mirza, M., Xu, B., Warde-Farley, D., Ozair, S., Courville, A., Bengio, Y, (2020), Generative adversarial nets. *Commun. ACM,* 63, 11, 139–144. https://doi.org/10.1145 /3422622.

[11] Isola, P., Zhu, J.Y., Zhou, T., Efros, A.A, (2017), Image-to-Image Translation with Conditional Adversarial Networks, *IEEE Conference on Computer Vision and Pattern Recognition (CVPR 2017),* Honolulu, USA, 5967-5976. https://doi.org/10.1109/CVPR.2017.632

[12] Karras, T., Aila, T., Laine, S., Lehtinen, J.: Progressive growing of GANs for improved quality, stability, and variation. ICLR (2018) *ArXiv preprint* https://arxiv.org/abs/ 1710.10196.

[13] Gatys, L.A., Ecker, A.S., Bethge, M., (2016), Image style transfer using convolutional neural

networks. *IEEE Conference on Computer Vision and Pattern Recognition (CVPR)*, Las Vegas, NV, USA, 2016, pp. 2414-2423, https://doi.org/10.1109/CVPR.2016.265.

[14] Sato M., Hotta K., Imanishi A., Matsuda M. and Terai K. (2018). Segmentation of Cell Membrane and Nucleus by Improving Pix2pix. *11th International Joint Conference on Biomedical Engineering Systems and Technologies (BIOSTEC 2018,)BIOSIGNALS, Vol. 4:* 216-220. https://doi.org/10.5220/0006648302160220.

[15] Zhu, J., Park, T., Isola, P., and Efros, A., (2017), Unpaired Image-to-Image Translation Using Cycle-Consistent Adversarial Networks," *IEEE International Conference on Computer Vision (ICCV 2017)*, Venice, Italy, pp. 2242-2251, https://doi.org/10.1109/ICCV.2017.244.

[16] Han, Z., Wei, B., Mercado, A., Leung, S., Li, S.: Spine-GAN: Semantic segmenta- tion of multiple spinal structures. *Medical image analysis* 50, 23–35 (2018)

[17] Dong, X., Lei, Y., Wang, T., Thomas, M., Tang, L., Curran, W.J., Liu, T., Yang, X.: Automatic multiorgan segmentation in thorax CT images using U-net-GAN. *Medical physics* 46(5), 2157–2168 (2019)

[18] He, K., Zhang, X., Ren, S., Sun, J.: Deep residual learning for image recognition. In: *Proceedings of the IEEE conference on computer vision and pattern recognition.* pp. 770–778 (2016)

[19] Nema, S., Dudhane, A., Murala, S., Naidu, S.: RescueNet: An unpaired GAN for brain tumor segmentation. *Biomedical Signal Processing and Control* 55, 101641 (2020)

[20] Yi, X., Walia, E., Babyn, P., (2019), Generative adversarial network in medical imaging: A review, *Medical Image Analysis*, Volume 58, 101552, ISSN 1361-8415, https://doi.org/10.1016/j.media.2019.101552.

[21] Alogna, E., Giacomello, E., and Loiacono, D., (2020) Brain Magnetic Resonance Imaging Generation using Generative Adversarial Networks, *IEEE Symposium Series on Computational Intelligence (SSCI)*, Canberra, ACT, Australia, 2020, pp. 2528-2535, https://doi.org/10.1109/SSCI47803.2020.9308244. .

[22] Cirillo, M., Abramian, D., Eklund, A. (2021). Vox2Vox: 3D-GAN for Brain Tumour Segmentation. *BrainLes2020, SpringerLNCS*. vol 12658. https://doi.org/10.1007/978-3-030-72084-1_25.

[23] Parmar, B., Parikh, M. (2021). Brain Tumor Segmentation and Survival Prediction Using Patch Based Modified 3D U-Net. BrainLes 2020. *SpringerLNCS*, vol 12659. https://doi.org/10.1007/978-3-030-72087-2_35

[24] Li, C., Wand, M. (2016). Precomputed Real-Time Texture Synthesis with Markovian Generative Adversarial Networks. *Computer Vision, ECCV 2016. SpringerLNCS*. vol 9907. https://doi.org/10.1007/978-3-319-46487-9_43

[25] Menze, B.H., Jakab, A., Bauer, S., Kalpathy-Cramer, J., Farahani, K., Kirby, J., Burren, Y., Porz, N., Slotboom, J., Wiest, R., et al.: The multimodal brain tumor image segmentation benchmark (BRATS*). IEEE transactions on medical imaging*, 34(10), 1993–2024 (2014)

[26] S. Bakas, H. Akbari, A. Sotiras, M. Bilello, M. Rozycki, J. Kirby, et al., "Segmentation Labels and Radiomic Features for the Pre-operative Scans of the TCGA-GBM collection", *The Cancer Imaging Archive,* 2017. https://doi.org/10.7937/K9/TCIA.2017.KLXWJJ1Q

[27] S. Bakas, H. Akbari, A. Sotiras, M. Bilello, M. Rozycki, J. Kirby, et al.,(opens in a new window) "Segmentation Labels and Radiomic Features for the Pre-operative Scans of the TCGA-LGG collection", *The Cancer Imaging Archive,* 2017. https://doi.org/10.7937/K9/TCIA.2017.GJQ7R0EF

[28] Bakas, S., Akbari, H., Sotiras, A., Bilello, M., Rozycki, M., Kirby, J.S., Freymann, J.B., Farahani, K., Davatzikos, C.: Advancing the cancer genome atlas glioma MRI collections with expert segmentation labels and radiomic features. *Scientific data* 4, 170117 (2017)

[29] Bakas, S., Reyes, M., Jakab, A., Bauer, S., Rempfler, M., Crimi, A., Shinohara, R.T., Berger, C., Ha, S.M., Rozycki, M., et al.: Identifying the best machine learning algorithms for brain tumor segmentation, progression assessment, and over- all survival prediction in the BRATS challenge. *arXiv preprint* arXiv:1811.02629 (2018)

[30] Tustison, N. J., Avants, B. B., Cook, P. A., Zheng, Y., Egan, A., Yushkevich, P. A., & Gee, J. C. (2010). N4ITK: improved N3 bias correction. *IEEE transactions on medical imaging*, *29*(6), 1310–1320. https://doi.org/10.1109/TMI.2010.2046908

[31] Paszke, Adam et al. "Automatic differentiation in PyTorch," *NIPS-W* 2017.

[32] 26.D. Jha et al., "ResUNet++: An Advanced Architecture for Medical Image Segmentation," *2019 IEEE International Symposium on Multimedia (ISM), San Diego, CA, USA,* 2019, pp. 225-2255, https://doi.org/10.1109/ISM46123.2019.00 049.

[33] A. Ng, "Gradient descent in practice I - feature scaling," Coursera. [Online]. Available: https://www.coursera.org/learn/machine-learning /lecture/xx3Da/gradient-descent-in-practice-i-feature-scaling

[34] "Psnr," Mathworks. [Online]. Available: https://it. Mathworks.com/help/vision/ref/psnr.html

[35] Z. Wang, A. Bovik, H. Sheikh, and E. Simoncelli, "Image quality assessment: From error visibility to structural similarity," *Image Processing, IEEE Transactions on*, vol. 13, pp. 600 – 612, 05 2004. [Online]. Available: https://ieeexplore.ieee.org/document/1284395